

Paper for Journal of Geophysical Research

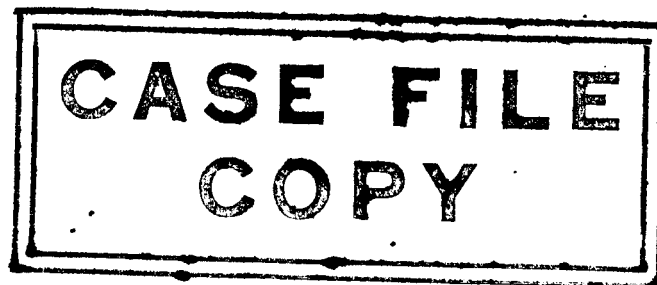
THEORETICAL DETERMINATION OF THE BOUNDARY OF THE  
GEOMAGNETIC FIELD IN A STEADY SOLAR WIND

By Benjamin R. Briggs\* and John R. Spreiter\*

National Aeronautics and Space Administration  
Ames Research Center  
Moffett Field, Calif.

ABSTRACT

The interaction of the geomagnetic field and a neutral ionized corpuscular solar stream is investigated. According to the theory of Chapman and Ferraro, the interaction is such that the geomagnetic field is confined to the interior of a cavity in the stream into which the particles of the stream do not penetrate. An approximate solution is presented for the complete shape of the boundary of the geomagnetic field for the case where the magnetic dipole axis is normal to the free-stream velocity vector. The calculations were made with the aid of an IBM 7090 electronic computer.



---

\*Research Scientist

12565  
22 p. 173: 8.2.60 ph. 80.86 ref.

## INTRODUCTION

It is generally believed (see, e.g., Chapman [1960], Ferraro [1960a], and Dungey [1958] for recent accounts) that the earth's magnetic field does not extend infinitely in all directions, but is bounded on the sunward side as a result of its interaction with a neutral ionized stream of particles emanating from the sun. (Dissenting views have been summarized by Alfvén [1961].) The interaction of the neutral solar stream with the geomagnetic field is such, according to the theory of Chapman and Ferraro, that the field is confined to the interior of a cavity in the stream into which the particles of the stream do not penetrate. Although much of the earlier work is concerned with the manner in which the boundary forms and evolves (see Ferraro [1960a] and Chapman and Kendall [1961] for recent developments), the present paper is concerned with the determination of the ultimate shape and location of the boundary for the idealized case in which the earth is deeply immersed in a uniform steady stream.

The steady-state Chapman-Ferraro problem is formulated in the following way. The magnetic field inside the boundary is considered to consist of the geomagnetic dipole field plus a component induced by electric currents in the boundary. It is supposed that the component of the total field normal to the boundary vanishes, and that the square of the total (tangential) field intensity at the boundary is proportional to the normal component of the momentum of the incident solar particles. The shape and location of the boundary and the total magnetic field inside it are then given by that solution of the magnetic field equations which satisfies the stated boundary conditions. The exact solution has not been given for this problem in three

dimensions, but the corresponding problem in two dimensions has been solved analytically by Zhigulev and Romishevskii [1959], Hurley [1961], and Dungey [1961].

Beard [1960] simplified the three-dimensional problem by relinquishing the condition that the component of the total magnetic field normal to the boundary vanishes, and applying instead the approximation that the magnetic field at the boundary is two times the tangential component of the dipole field. He then used a power series technique to calculate the shape of the boundary of the geomagnetic field on the daytime side, for the case where the dipole axis is perpendicular to the free-stream velocity vector.

Spreiter and Briggs [1961, 1962a, 1962b] employed a similar analysis and calculated traces of the boundary in the plane of the dipole axis and free-stream velocity vector for arbitrary inclinations of the dipole axis. They used the related approximation, suggested by Ferraro [1960b], that the total magnetic field at the boundary is  $2f$  times the tangential component of the dipole field, where  $f$  is a constant. No information was supplied concerning the proper value for  $f$  in the three-dimensional problem. It was shown, however, that the distance along the sun-earth line to the boundary in the corresponding approximate two-dimensional problem is about 5 percent too large if  $f$  is unity. If  $f$  is taken to be 0.91, the coordinates of the entire approximate boundary agree well with the results indicated by the exact two-dimensional solutions cited in the foregoing paragraph.

The present work is an extension of that done by Beard [1960], and Spreiter and Briggs [1961, 1962a, 1962b]. The coordinates of the entire boundary of the geomagnetic field are calculated for the case in which the dipole axis is perpendicular to the free-stream velocity vector. The mathematical derivations have been given by the authors cited here and are not repeated in the present paper. The notation used by Spreiter and Briggs is retained for convenience.

It may be observed that the dimensions of the boundary, as calculated here using representative stream conditions, are much smaller than have been inferred from the magnetometer experiments of Pioneer I and Pioneer V. (See Sonett, et al. [1960], and Coleman, et al. [1960].) The dimensions of the boundary can be increased by substantially decreasing the velocity or number density of protons in the solar stream; or, as has been indicated by Spreiter and Briggs [1961, 1962a], by the inclusion in the theoretical model of a ring current as has been proposed by Smith, et al. [1960] on the basis of data from Explorer VI and Pioneer V. The effect of a ring current has not been considered in the present calculations. It is expected, however, in the light of results given by Spreiter and Alksne [1962], that the general features of the shape of the boundary would not be greatly affected by inclusion of a ring current, but that the dimensions of the boundary would be increased considerably.

## MATHEMATICAL FORMULATION OF THE PROBLEM

### Preliminary Discussion

The determination of the shape of the boundary of the geomagnetic field, and the total magnetic field  $\underline{H}$  inside it, involves the solution of the magnetic field equations  $\text{div } \underline{H} = 0$  and  $\text{curl } \underline{H} = 0$ . The earth's

magnetic field is represented by a three-dimensional dipole singularity at the origin (the center of the earth). The normal component of  $\underline{H}$  vanishes at the boundary, and Dungey [1958] has shown (see Spreiter and Briggs [1962b] for clarification of contrary views expressed in Spreiter and Briggs [1961a]) that the total (tangential) field at the boundary,  $H_s$ , may be expressed mathematically by the relation

$$\frac{H_s^2}{8\pi} = 2mnv^2 \cos^2 \psi \quad (1)$$

The quantities  $m$ ,  $n$ , and  $v$  are mass, number density, and velocity of the protons of the solar stream, and  $\psi$  is the angle between the free-stream velocity vector and an outward normal to the surface. The condition  $\cos \psi \leq 0$  must hold on the boundary.

It is a property of the boundary value problem described above that the field  $\underline{H}$  can vanish only at isolated points on the boundary. These points are designated neutral points. It follows from equation (1) that  $\cos \psi$  vanishes, and the boundary is therefore parallel to the stream, at these points.

Beard [1960] dropped the condition that the normal component of  $\underline{H}$  vanishes at the boundary and replaced it with the approximate condition that  $H_s = 2H_t$ , where  $H_t$  is the tangential component of the geomagnetic dipole field  $\underline{H}_p$  at the boundary. The closely related approximation, suggested by Ferraro [1960b],

$$H_s = 2fH_t \quad (2)$$

where  $f$  is a constant, was used by Spreiter and Briggs [1961, 1962a, 1962b] and is employed in the present work.

The differential equation that defines, approximately, the shape of the boundary is obtained by substitution of equation (2) into equation (1). For the case where the dipole axis is normal to the free-stream velocity vector, it is

$$\pm \frac{\left( \sin \theta + \frac{2 \cos \theta}{\rho} \frac{\partial \rho}{\partial \theta} \right)}{\rho^3 \left[ 1 + \left( \frac{1}{\rho} \frac{\partial \rho}{\partial \theta} \right)^2 \right]^{1/2}} = \frac{\left( \sin \varphi \sin \theta - \frac{\sin \varphi \cos \theta}{\rho} \frac{\partial \rho}{\partial \theta} - \frac{\cos \varphi}{\rho \sin \theta} \frac{\partial \rho}{\partial \varphi} \right)}{\left[ 1 + \left( \frac{1}{\rho} \frac{\partial \rho}{\partial \theta} \right)^2 + \left( \frac{1}{\rho \sin \theta} \frac{\partial \rho}{\partial \varphi} \right)^2 \right]^{1/2}} \quad (3)$$

where  $\rho = r/r_0$  and

$$r_0 = \left( \frac{4f^2 M_p^2}{16\pi m v^2} \right)^{1/3} = a \left( \frac{4f^2 H_{p_0}^2}{16\pi m v^2} \right)^{1/3} \quad (4)$$

The variables  $r$ ,  $\theta$ , and  $\varphi$  are spherical coordinates that are fixed with respect to the geomagnetic dipole axis (see fig. 1). The quantity  $M_p$ , the magnetic moment of the dipole, is equal to  $a^3 H_{p_0}$ , where  $a$  represents the radius of the earth, and  $H_{p_0}$  is the magnitude of  $H_p$  at the magnetic equator on the surface of the earth. The quantities in equation (4) are in cgs units, and numerical values for  $a$ ,  $H_{p_0}$ , and  $m$  are  $6.37 \times 10^8$  cm, 0.312 gauss, and  $1.67 \times 10^{-24}$  gram, respectively.

The quantity  $r_0$  is the geocentric distance along the sun-earth line to the boundary of the geomagnetic field. The effect of variations of  $n$  and  $v$  on  $r_0$  is shown in figure 2 for two values of the constant  $f$ . Representative values of  $v$  and  $n$  are 500 km/sec and 10 protons/cm<sup>3</sup>. These lead to values for  $r_0$  of 7.6 earth radii for  $f = 1$  and 6.9 earth radii for  $f = 0.75$ .

If attention is confined to the plane  $\varphi = \pm\pi/2$  ( $x = 0$ ) where the derivative  $\partial\rho/\partial\varphi$  is zero by consideration of symmetry, equation (3)

reduces to an ordinary differential equation that can be solved analytically. The trace of the boundary in this plane is illustrated in figure 3. The front portion is circular,  $\rho = 1$ , and the upper portion is defined by the relation  $\rho \cos \theta = (3/2^{2/3})\rho^3/(1 + \rho^3)$ .

The problem in three dimensions is to find the solution of equation (3) whose trace in the plane  $\varphi = \pm\pi/2$  is as shown in figure 3. It will be seen, subsequently, that the boundary in the upper half-space ( $z \geq 0$ ) is composed of two intersecting surfaces. One will be called the main surface. It contains the circular trace  $\rho = 1$ , and that portion of the upper trace that lies in the half-plane  $\varphi = -\pi/2$  (i.e.,  $z > 0, y \leq 0$ ). The other, to be called the polar surface, contains the small portion of the upper trace that lies in the half-plane  $\varphi = \pi/2$  (i.e.,  $z > 0, y \geq 0$ ). This segment of the upper trace is indicated by broken lines in figure 3. The coordinates of the boundary of the geomagnetic field are then determined by solving the initial value problem defined by equation (3) together with the traces of the solution in the plane  $\varphi = \pi/2$ .

Equation (3) may be put into a form that renders it more amenable to standard numerical procedures by solving for the derivative  $\partial\rho/\partial\varphi$ ; that is,

$$\frac{\partial\rho}{\partial\varphi} = \rho \sin \theta \left[ \frac{-\sin \varphi \cos \varphi F_1 - F_2 \sqrt{\frac{F_1^2 \sin^2 \varphi}{F_3} - \left(\frac{F_2^2}{F_3} - \cos^2 \varphi\right)}}{\left(\frac{F_2^2}{F_3} - \cos^2 \varphi\right)} \right] \quad (5)$$

The functions  $F_1, F_2,$  and  $F_3$  are

$$\left. \begin{aligned} F_1 &= \sin \theta - \frac{\cos \theta}{\rho} \frac{\partial \rho}{\partial \theta} \\ F_2 &= \frac{1}{\rho^3} \left( \sin \theta + \frac{2 \cos \theta}{\rho} \frac{\partial \rho}{\partial \theta} \right) \\ F_3 &= 1 + \left( \frac{1}{\rho} \frac{\partial \rho}{\partial \theta} \right)^2 \end{aligned} \right\} \quad (6)$$

The numerical integration of equation (5) is discussed in the next section.

### NUMERICAL INTEGRATION

The coordinates of the two portions of the boundary of the geomagnetic field are determined by forward integration from the traces in the plane  $\varphi = \pi/2$  toward larger values of  $\varphi$ . The variable  $\rho$  is extrapolated over intervals  $\Delta\varphi$  in surfaces of constant  $\theta$  by use of an iterative extrapolation process based on Euler's method for solving ordinary differential equations. (See, e.g., Kunz [1957].) Equation (5) is used to calculate the derivatives  $\partial\rho/\partial\varphi$  and at each new value of  $\varphi$ ,  $\partial\rho/\partial\theta$  is evaluated by numerical differentiation.

The initial step away from the plane  $\varphi = \pi/2$  is effected by means of the truncated series

$$\begin{aligned} \rho &= \rho_0 + \Delta\varphi(\partial\rho/\partial\varphi)_0 + \frac{\Delta\varphi^2}{2} (\partial^2\rho/\partial\varphi^2)_0 + \dots \\ &\approx \rho_0(1 + \alpha \Delta\varphi^2) \end{aligned} \quad (7)$$

which is similar to the one used by Beard [1960]. Here  $\rho_0$  represents the trace of the boundary in the plane of  $\varphi = \pi/2$ . The constant  $\alpha = \alpha(\theta)$ , which is proportional to the second derivative of  $\rho$  with respect to  $\varphi$ ,



is evaluated by substituting equation (7) into equation (5). It develops that  $\alpha$  is a solution of the quadratic equation

$$\frac{f_2^2}{f_3 \sin^2 \theta} \alpha^2 - \left[ \frac{f_1}{\sin \theta} + \frac{f_2}{2} \left( 3f_2 + \frac{2\delta_0}{\rho_0^4} \cos \theta \right) + \frac{f_1 \delta_0}{2\rho_0} \cos \theta \right] \alpha + \frac{f_1^2}{4} = 0 \quad (8)$$

where  $\delta_0 = (\partial\rho/\partial\theta)_{\varphi=\pi/2}$ , and the functions  $f_1$ ,  $f_2$ , and  $F_3$  are simply  $F_1$ ,  $F_2$ , and  $F_3$  (eqs. (6)) evaluated at  $\varphi = \pi/2$ . In the case of the main surface, where  $\rho_0 = 1$  and  $\delta_0 = 0$ , the desired solution of equation (8) is

$$\alpha = \frac{1}{4} \left[ (2 + 3 \sin^2 \theta) - \sqrt{(2 + 3 \sin^2 \theta)^2 - 4 \sin^2 \theta} \right] \quad (9)$$

After  $\alpha$  is computed by means of equation (8), the values for  $\rho$  at  $\varphi = \pi/2 + \Delta\varphi$  are readily calculated by means of equation (7). The derivative  $\partial\rho/\partial\varphi$  here is simply  $2\alpha\rho_0 \Delta\varphi$ , and  $\partial\rho/\partial\theta$  may now be calculated by numerical differentiation. Thus the trace of the boundary, as well as its derivatives, is completely determined in the plane  $\varphi = \pi/2 + \Delta\varphi$ .

The integration process for succeeding intervals proceeds in the following fashion: The values for  $\rho$  and  $\partial\rho/\partial\varphi$  at station  $\varphi_i$  are inserted in the linear extrapolation formula

$$\rho_{i+1} = \rho_i + \Delta\varphi(\partial\rho/\partial\varphi)_i \quad (10)$$

in order to get a first estimate for  $\rho$  at station  $\varphi_{i+1} = \varphi_i + \Delta\varphi$ . The derivative  $(\partial\rho/\partial\theta)_{i+1}$  is computed by numerical differentiation, and then equation (5) is used to evaluate the derivative  $(\partial\rho/\partial\varphi)_{i+1}$ . Finally a refined value for  $\rho_{i+1}$  is determined by means of the iterative extrapolation formula

$$\rho_{i+1} = \rho_i + (\Delta\varphi/2) \left[ (\partial\rho/\partial\varphi)_i + (\partial\rho/\partial\varphi)_{i+1} \right] \quad (11)$$

The derivatives  $(\partial\rho/\partial\theta)_{i+1}$  and  $(\partial\rho/\partial\varphi)_{i+1}$  are now recomputed as before, and the process is repeated from equation (10) to integrate over the next increment  $\Delta\varphi$ .

The forward integration technique outlined here has been used to find the coordinates of traces of the boundary of the geomagnetic field in planes  $\varphi = \text{constant}$  in the range  $\pi/2 \leq \varphi < 3\pi/2$  and  $0 \leq \theta \leq \pi/2$ . This range of values of  $\varphi$  and  $\theta$  is sufficient by reasons of symmetry to establish the entire boundary. In any plane  $\varphi = \text{constant}$  the traces of the two surfaces intersect, and the boundary is defined by the exterior portion of the intersecting traces.

#### RESULTS AND DISCUSSION

The coordinates of the main and polar surfaces have been calculated at  $5^\circ$  intervals of  $\varphi$  in the range  $90^\circ \leq \varphi \leq 270^\circ$ . The increment and range of variation of  $\theta$  were  $5^\circ$  and  $0 \leq \theta \leq 140^\circ$  in the case of the main surface, and  $2^\circ$  and  $0 \leq \theta \leq 30^\circ$  in the case of the polar surface. It is clear that the main surface possesses mirror symmetry in the equatorial plane, and it will be seen subsequently that the range of interest of  $\theta$  in the polar surface is  $0 \leq \theta < 20^\circ$ . The calculations were carried out beyond the range of interest of the variable  $\theta$  for both surfaces, however, in order to minimize the effects of end-point inaccuracy inherent in the procedure used to evaluate the derivative  $\partial\rho/\partial\theta$  in planes of constant  $\varphi$ . It may be observed that the results do not change significantly with the use of increments somewhat larger or smaller than those employed here.

It develops that the numerical technique described in the foregoing section is not adequate for calculating the coordinates of the main surface near the plane  $\varphi = 270^\circ$ . The derivative  $\partial\rho/\partial\varphi$  becomes excessively large in this region, with the chosen mesh size, and therefore the extrapolation process is not sufficiently accurate. The procedure works well up to  $\varphi = 255^\circ$ , however, and these results along with the known analytic solution in the plane  $\varphi = 270^\circ$  (see fig. 3), are sufficient to determine the entire boundary.

The numerical results are presented graphically in figures 4 and 5. Figure 4 shows traces of the boundary of the geomagnetic field in the planes  $\varphi = 90^\circ, 105^\circ, 120^\circ, \dots, 270^\circ$ . The trace for the plane  $\varphi = 270^\circ$  is the analytic solution as given in figure 3. Figure 5 is an isometric view of the boundary. The curve designated S in this figure represents the intersection of the main and polar surfaces, and the point labeled N corresponds to the neutral point in the exact solution.

It is of interest to examine the deterioration of the results with the introduction of certain simplifications in the integration procedure. It is found, for example, that the power series starting process may be omitted with no major effect on the results. A comparison is shown in figure 6(a) of calculations made with and without the starting series. The differences are seen to be confined essentially to traces of the main surface. If, on the other hand, equation (11) is deleted, then the extrapolation process is purely linear. A comparison is shown in figure 6(b) of calculations made with the full iterative process, and the linear process with and without the starting series. It is seen that if the starting series is retained, linear

extrapolation produces results that are in substantial agreement with the results obtained using the iterative process. If, on the other hand, the starting series is dropped, the linear process yields irregular results that would probably be regarded as unsatisfactory for most purposes.

The present results may be compared with those given by Beard [1960]. Traces of the boundary in planes  $90^\circ \leq \varphi \leq 180^\circ$  are reproduced in figure 7, and Beard's results are indicated by broken lines. It is seen that the two sets of computations agree well except in a region near the polar axis. These differences result from corresponding differences in the trace of the boundary in the meridian plane  $\varphi = 90^\circ$  that have been discussed previously by Spreiter and Briggs [1961, 1962a, 1962b]. Beard has informed the present authors privately that the latter differences result from the fact that the present authors base their analysis on the consistent use of the approximation given by equation (2), whereas he uses another approximation in the vicinity of the polar axis. Beard, and also Spreiter and Briggs [1961], have in addition made refined calculations for the trace in the equatorial plane by solving the ordinary differential equation that results when  $\theta$  is set equal to  $90^\circ$  and  $\partial\rho/\partial\theta$  to zero in equation (5). These results are in almost perfect agreement with the present calculations.

As noted in the introduction, Spreiter and Briggs [1961, 1962a, 1962b] showed that the coordinates of the boundary given by the exact and approximate solutions of the two-dimensional Chapman-Ferraro problem can be brought into close agreement if the value for the constant  $f$  is taken to be 0.91. The principal remaining difference is that the discontinuous slope in the vicinity of the neutral point in the approximate solution appears as a smoothly turning

curve in the exact solution. The exact solution has not been given for the three-dimensional problem, but according to an estimate of Beard [1960] the geocentric distance on the sunward side to the approximate boundary is too great by about 7 to 11 percent. A major portion of this discrepancy can be rectified if  $f$  is chosen in the range 0.7 to 0.8. There remains, however, the discrepancy associated with the discontinuity of slope along the curve of intersection of the main and polar surfaces.

In the exact solution of the Chapman-Ferraro problem, the field strength is small in the vicinity of the neutral point, and vanishes at the neutral point. It follows from equation (1) that the slope of the boundary with respect to the free-stream direction is small in this region, also. These remarks apply to the approximate solution as well, except that the field strength does not vanish at the point that corresponds to the neutral point. Although the percentage errors may be large, the absolute magnitude of the errors in slope should be small or moderate. These errors would tend, in any case, to be of secondary importance since the coordinates of the boundary are calculated by a process involving the integration of surface slopes. It is anticipated, therefore, that the discontinuous slope along the curve  $S$  represents a local failure of the approximate method of solution of the problem. It is concluded, however, that with the appropriate choice for the value of the constant  $f$ , the coordinates of the approximate boundary should be in substantial agreement with the coordinates that would be given by the exact solution of the Chapman-Ferraro problem.

REFERENCES

- Alfvén, H., Commission de la magneto-hydrodynamique et de la physique des gaz ionisés. IAU 11th general assembly agenda and draft reports. 499-520, June, 1961.
- Beard, David B., The interaction of the terrestrial magnetic field with the solar corpuscular radiation. *J. Geophys. Research*, 65, 3559-3568, 1960.
- Chapman, Sydney, Idealized problems of plasma dynamics relating to geomagnetic storms. *Reviews Modern Physics*, 32, 919-933, 1960.
- Chapman, S., and P. C. Kendall, An idealized problem of plasma dynamics that bears on geomagnetic storm theory; oblique projection. *J. Atmospheric and Terrest. Physics*, 22, 142-156, 1961.
- Coleman, P. J., Jr., C. P. Sonett, D. L. Judge, and E. J. Smith, Some preliminary results of the Pioneer V magnetometer experiment. *J. Geophys. Research*, 65, 1856-1857, 1960.
- Dungey, J. W., *Cosmic electrodynamics*. Cambridge University Press, Cambridge, 183 pp., 1958.
- Dungey, J. W., The steady state of the Chapman-Ferraro problem in two dimensions. *J. Geophys. Research*, 66, 1043-1047, 1961.
- Ferraro, V. C. A., Theory of sudden commencements and of the first phase of a magnetic storm. *Reviews Modern Physics*, 32, 934-940, 1960a.
- Ferraro, V. C. A., An approximate method of estimating the size and shape of the stationary hollow carved out in a neutral ionized stream of corpuscles impinging on the geomagnetic field. *J. Geophys. Research*, 65, 3951-3953, 1960b.
- Hurley, James, Interaction of a streaming plasma with the magnetic field of a two-dimensional dipole. *Phys. Fluids*, 4, 854-859, 1961.

- Kunz, Kaiser S., Numerical analysis. McGraw-Hill Book Co., Inc., New York, 381 pp., 1957.
- Smith, E. J., P. J. Coleman, D. L. Judge, and C. P. Sonett, Characteristics of the extraterrestrial current system: Explorer VI and Pioneer V. J. Geophys. Research, 65, 1858-1861, 1960.
- Sonett, C. P., D. L. Judge, A. R. Sims, and J. M. Kelso, A radial rocket survey of the distant geomagnetic field. J. Geophys. Research, 65, 55-68, 1960.
- Spreiter, John R., and Alberta Y. Alksne, On the effects of a ring current on the terminal shape of the geomagnetic field. J. Geophys. Research, 67, 1962.
- Spreiter, John R., and Benjamin R. Briggs, Theoretical determination of the form of the hollow produced in the solar corpuscular stream by interaction with the magnetic dipole field of the earth. NASA TR R-120, 1961.
- Spreiter, John R., and Benjamin R. Briggs, Theoretical determination of the form of the boundary of the solar corpuscular stream produced by interaction with the magnetic dipole of the earth. J. Geophys. Research, 67, 37-51, 1962a.
- Spreiter, John R., and Benjamin R. Briggs, On the choice of condition to apply at the boundary of the geomagnetic field in the steady-state Chapman-Ferraro problem. J. Geophys. Research, 67, 1962b.
- Zhigulev, V. N., and E. A. Romishevskii, Concerning the interaction of currents flowing in a conducting medium with the earth's magnetic field. Doklady Akad. Nauk. SSSR, 127, 1001-1004, 1959. [English translation: Soviet Physics - Doklady 4, 859-862, 1960.]

## Figure Legends

Fig. 1.- The coordinate systems.

Fig. 2.- Values of  $r_0$  for various velocities and number densities of the solar stream.

Fig. 3.- Analytic solutions in the plane  $\varphi = \pm\pi/2$ .

Fig. 4.- Traces of the boundary of the geomagnetic field in planes of constant  $\varphi$ .

Fig. 5.- Isometric view of the boundary of the geomagnetic field.

Fig. 6.- Comparisons of results obtained by iterative and linear extrapolation processes with and without the starting series.

Fig. 7.- Comparison with Beard's results.



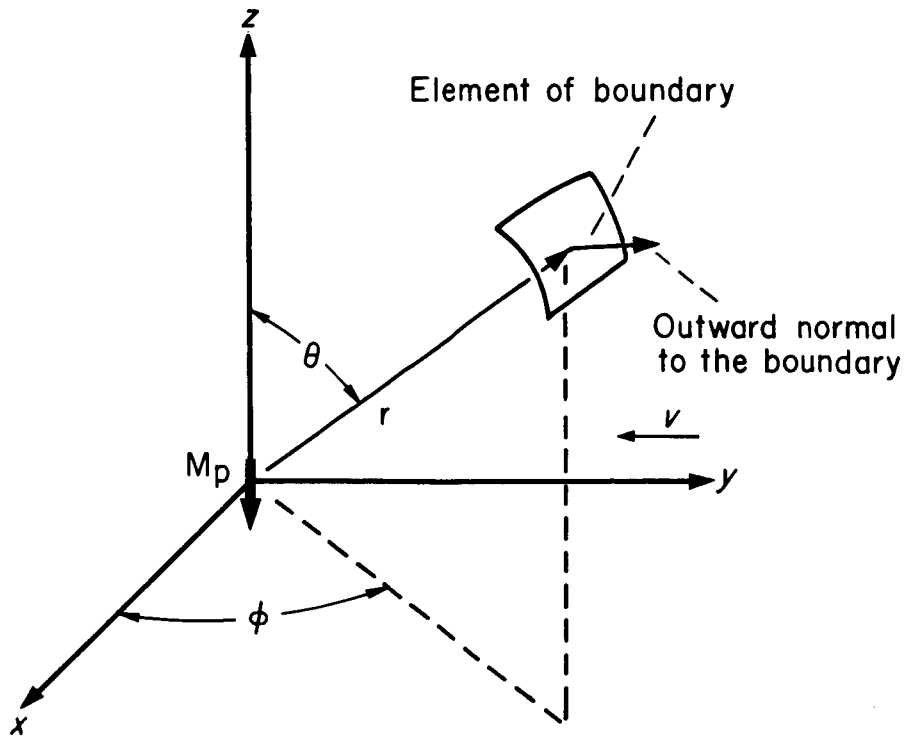


Figure 1.

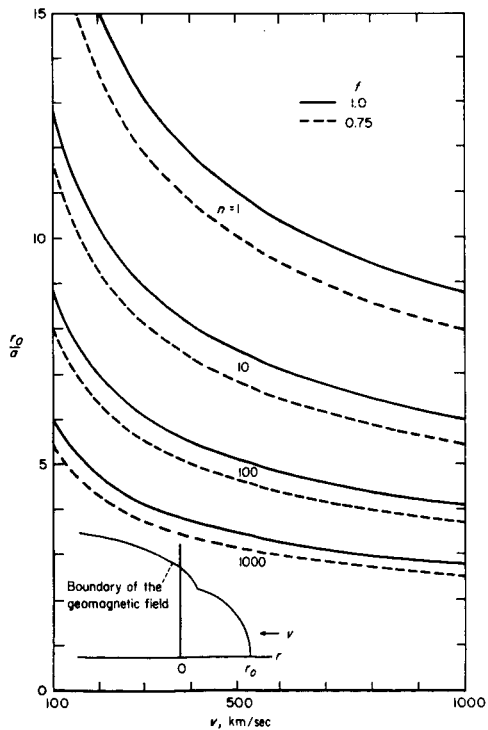


Figure 2.

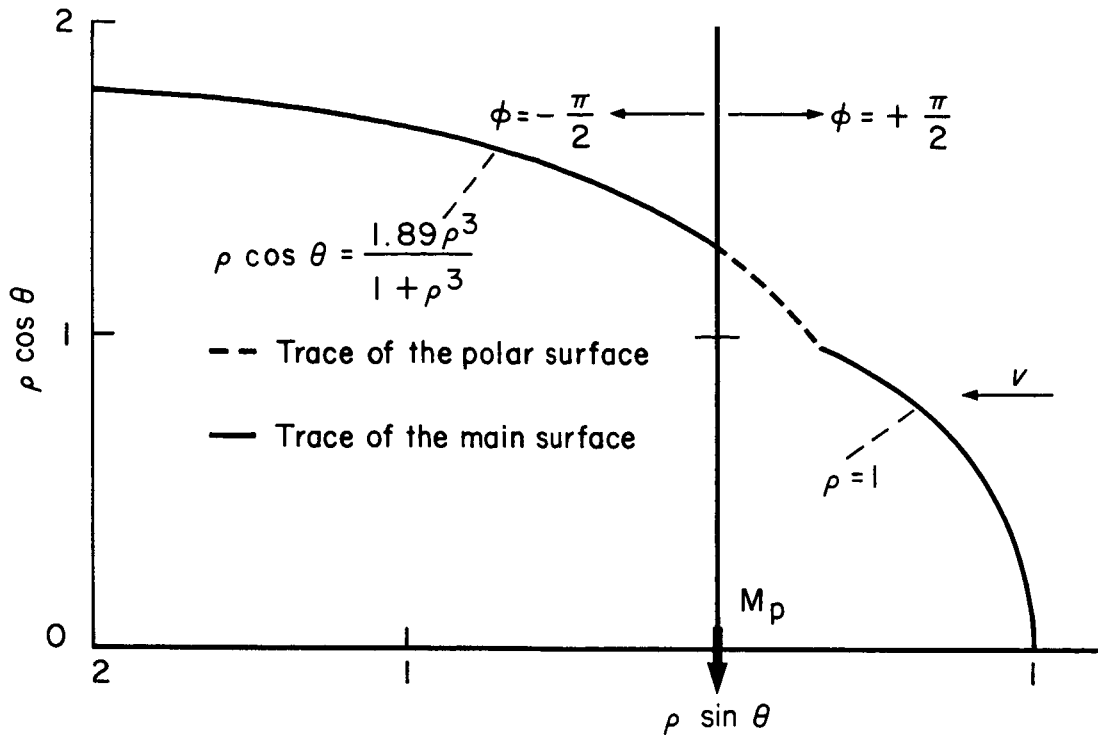


Figure 3.

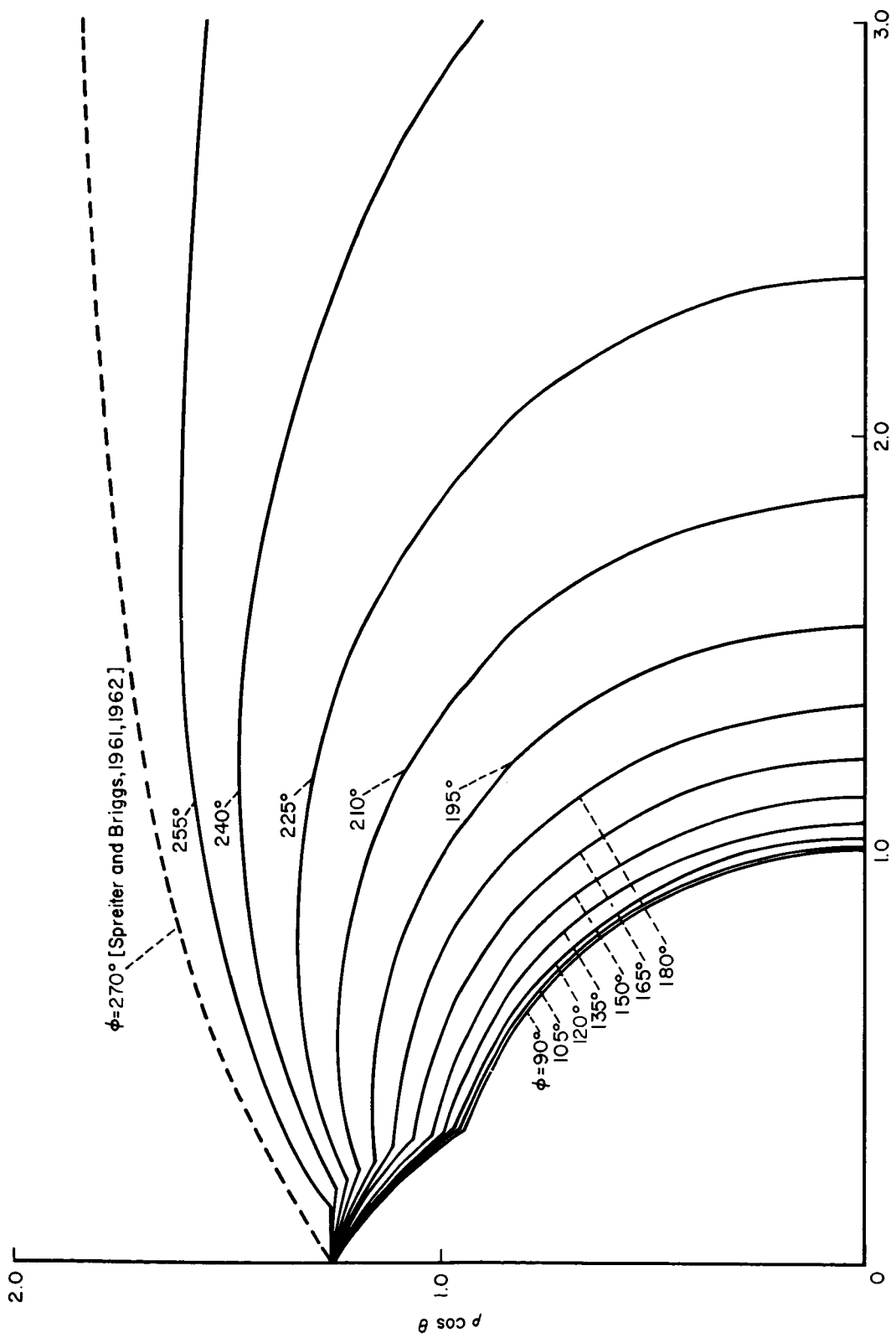


Figure 4.

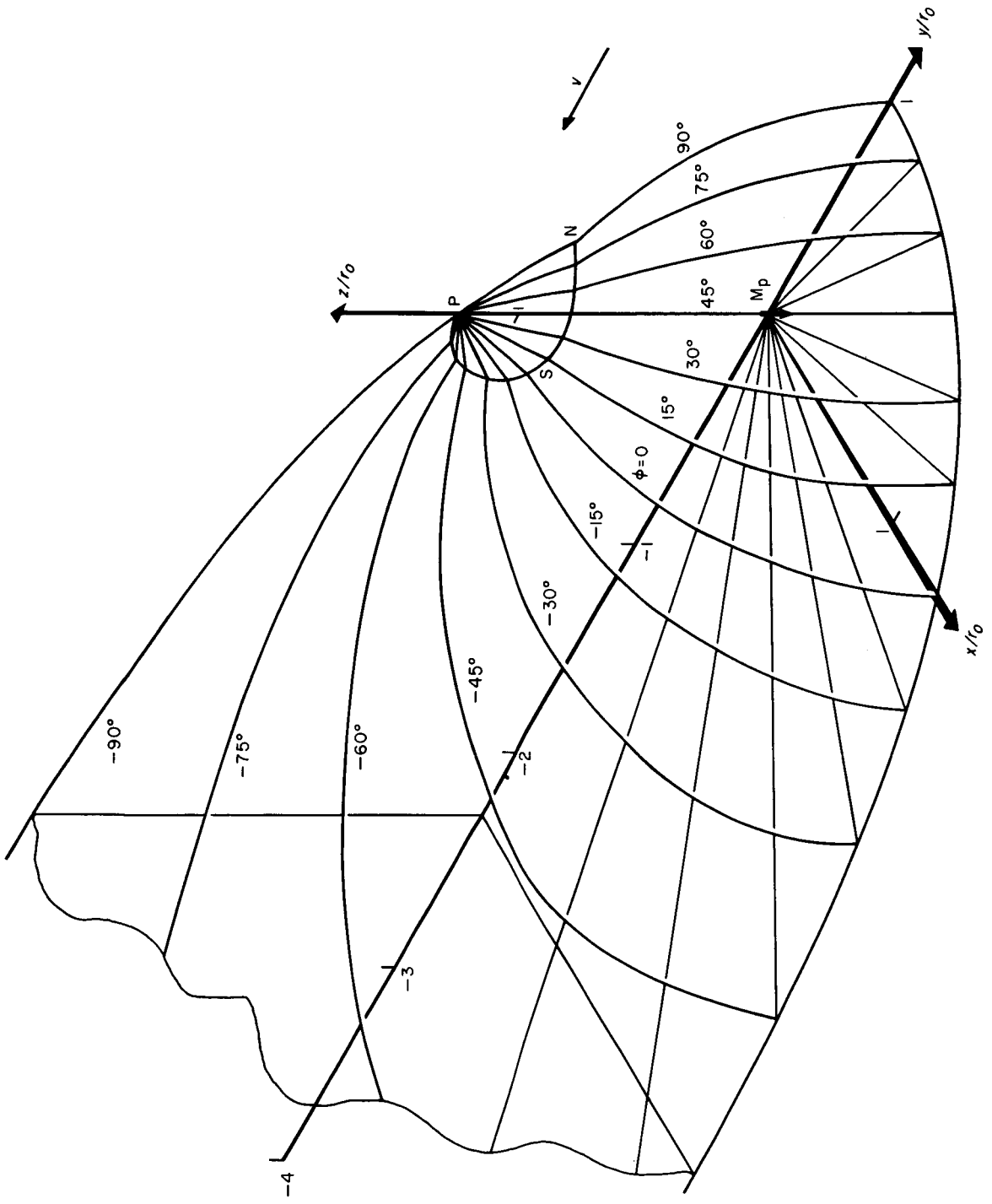


Figure 5.

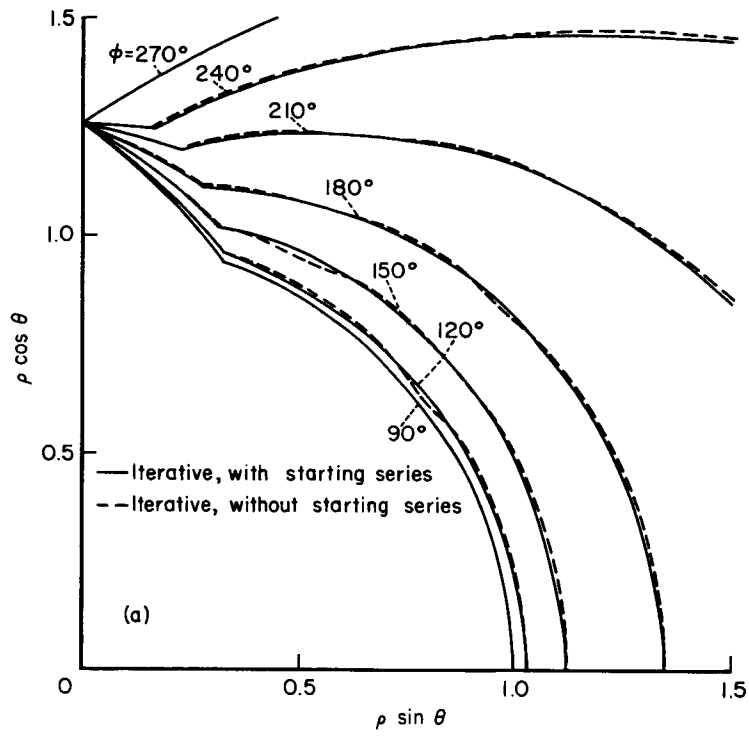


Figure 6(a).

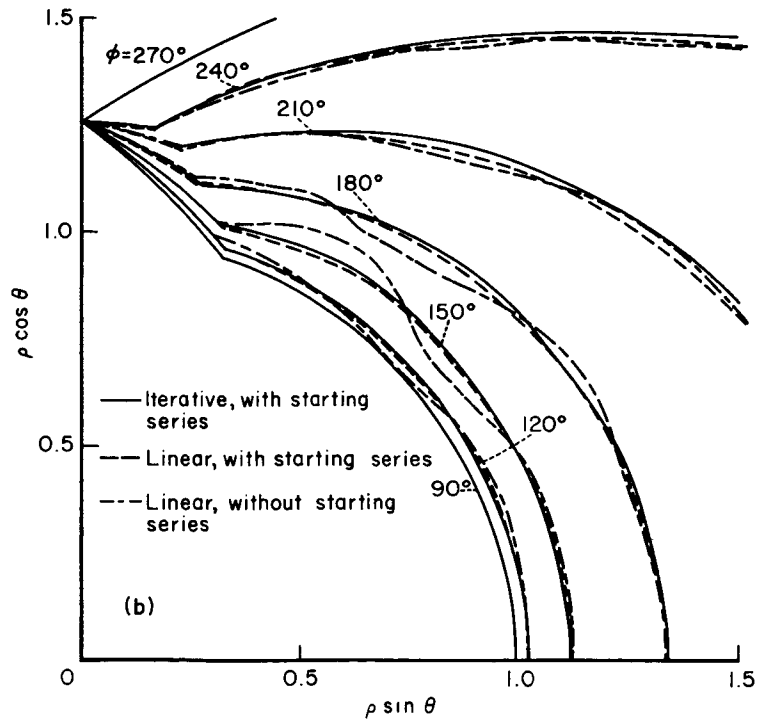


Figure 6(b).

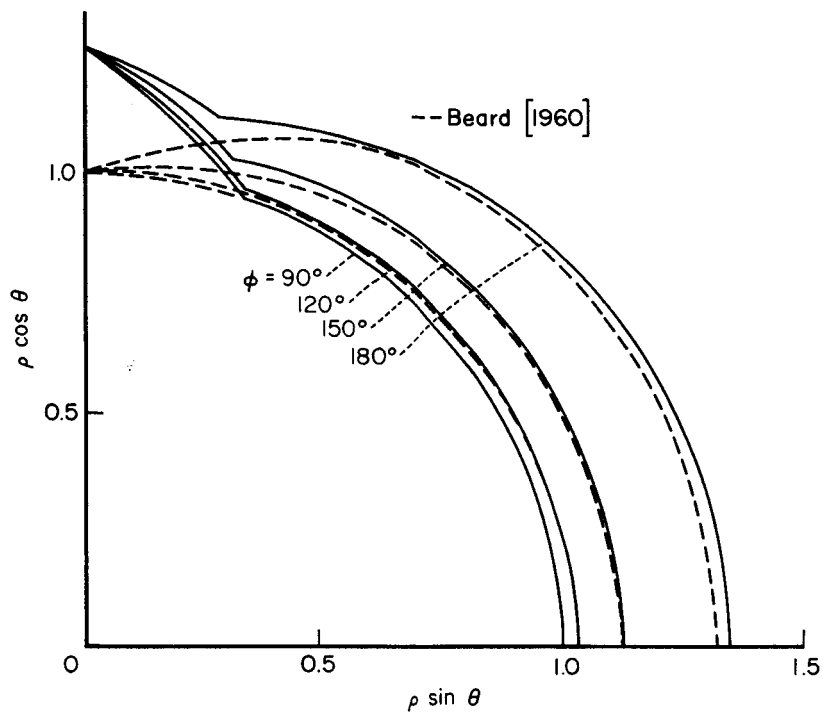


Figure 7.